

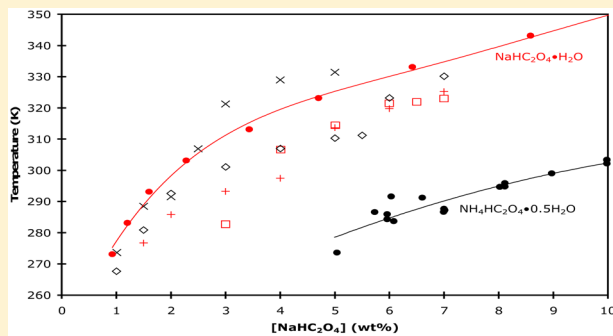
# Solubility of the Sodium and Ammonium Salts of Oxalic Acid in Water with Ammonium Sulfate

Lukas G. Buttke, Justin R. Schueller, Christian S. Pearson, and Keith D. Beyer\*

Department of Chemistry and Biochemistry, University of Wisconsin—La Crosse, La Crosse, Wisconsin 54601, United States

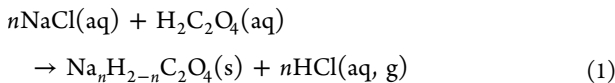
## Supporting Information

**ABSTRACT:** The solubility of the sodium and ammonium salts of oxalic acid in water with ammonium sulfate present has been studied using differential scanning calorimetry, X-ray crystallography, and infrared spectroscopy. The crystals that form from aqueous mixtures of ammonium sulfate/sodium hydrogen oxalate were determined to be sodium hydrogen oxalate monohydrate under low ammonium sulfate conditions and ammonium hydrogen oxalate hemihydrate under high ammonium sulfate conditions. Crystals from aqueous mixtures of ammonium sulfate/sodium oxalate were determined to be ammonium oxalate monohydrate under moderate to high ammonium sulfate concentrations and sodium oxalate under low ammonium sulfate concentrations. It was also found that ammonium sulfate enhances the solubility of the sodium oxalate salts (salting in effect) and decreases the solubility of the ammonium oxalate salts (salting out effect). In addition, a partial phase diagram for the ammonium hydrogen oxalate/water system was determined.



## INTRODUCTION

Field measurements of aerosols in the free and upper troposphere (UT) have shown that the major chemical components include sulfates, ammonium, organic species, and mineral dust,<sup>1,2</sup> with the most abundant inorganic components being ammonium and sulfate.<sup>3</sup> Among the organic components, dicarboxylic acids are present in aerosols in a range of environments especially for aerosols that have undergone chemical aging.<sup>4</sup> Dicarboxylic acids (DCAs) are found in primary organic aerosols as well as secondary organic aerosols,<sup>3</sup> and their concentration in aerosols is increasing.<sup>5</sup> Field measurements have shown that oxalic acid is the most abundant DCA in atmospheric aerosols.<sup>5–7</sup> Aerosols also commonly contain mineral dust whose components can be leached to the aqueous phase through chemical aging, especially under acidic conditions.<sup>8,9</sup> The metals at the surface or reacted to the aqueous phase of mineral dust particles can enhance the chemistry that occurs in the aqueous phase.<sup>8,10</sup> Field studies have shown an abundance of aerosols with organics and metals/metal salts from sea spray (Na, Mg),<sup>4,11–13</sup> biomass burning (K),<sup>14,15</sup> and mineral dusts/meteoritic material (Na, K, Ca, Fe).<sup>1,16–19</sup> Field and lab studies have shown that metal ions can displace hydrogen ions from organic acids to form carboxylate salts in atmospheric aerosols.<sup>11,13,20,21</sup> For example, for a particle with dissolved NaCl and oxalic acid that experienced UT temperatures and/or dry conditions, we would have



where  $n$  equals 1 or 2. Studies have shown that the HCl product is highly volatile, leaving behind an organic salt in the particle.<sup>13,20</sup> As the particle experiences cold/dry conditions in the atmosphere, the sodium oxalate salt could precipitate.<sup>21</sup> While the solubilities of  $\text{NaHC}_2\text{O}_4$  and  $\text{Na}_2\text{C}_2\text{O}_4$  in water have been known for some time,<sup>22,23</sup> the effect of ammonium sulfate on solubility in solutions of sodium oxalates has not been investigated. In particular, salts other than the sodium oxalates and ammonium sulfate could form from these complex solutions of ions. For example, Kissinger et al.<sup>24</sup> recently found that the least soluble solid in aqueous mixtures of sodium malonate or sodium hydrogen malonate and ammonium sulfate is sodium ammonium sulfate dihydrate (leontite). However, the sodium salts of oxalic acid are much less soluble in water than the sodium malonate salts, and thus, the effect of ammonium sulfate on their solubility needs investigation.

## EXPERIMENTAL SECTION

**Sample Preparation.** Solutions studied in DSC and FTIR experiments were made by mixing oxalic acid dihydrate (99+, Acros Organics), ammonium sulfate (99+, Sigma-Aldrich), and sodium hydroxide (beads, Fisher) with deionized water. For  $\text{NaHC}_2\text{O}_4$  samples, 1:1  $\text{NaOH}/\text{H}_2\text{C}_2\text{O}_4$  solutions were made, and for  $\text{Na}_2\text{C}_2\text{O}_4$ , 2:1  $\text{NaOH}/\text{H}_2\text{C}_2\text{O}_4$  solutions were made. For X-ray crystallography experiments, a single crystal was extracted from a saturated solution.

Received: May 23, 2016

Revised: July 27, 2016

Published: August 2, 2016

Table 1. Raw DSC and IR Data for Endothermic Transitions in  $(\text{NH}_4)_2\text{SO}_4/\text{NaHC}_2\text{O}_4$  Samples<sup>a</sup>

$[(\text{NH}_4)_2\text{SO}_4]$	$[\text{NaHC}_2\text{O}_4]$	mole ratio $(\text{NH}_4)_2\text{SO}_4/\text{NaHC}_2\text{O}_4$	ternary eutectic	ice melt	final salt dissolution	identity of final melting/dissolving compound
10.00	1.01	8.4	253.52	270.66		ice
10.00	2.01	4.2	253.48	270.53		ice
10.00	3.00	2.8	253.45	270.37	282.71	
10.00	4.01	2.1	253.34	270.18	306.63	$\text{NaHC}_2\text{O}_4\cdot\text{H}_2\text{O}$
10.01	5.01	1.7	253.34	270.18	314.40	$\text{NaHC}_2\text{O}_4\cdot\text{H}_2\text{O}$
10.00	6.00	1.4	253.42	270.31	321.41	$\text{NaHC}_2\text{O}_4\cdot\text{H}_2\text{O}$
10.00	6.50	1.3	253.52	270.29	321.91	$\text{NaHC}_2\text{O}_4\cdot\text{H}_2\text{O}$
10.00	7.00	1.2	253.44	270.03	322.99	$\text{NaHC}_2\text{O}_4\cdot\text{H}_2\text{O}$ <sup>b</sup>
20.01	1.00	17.0	253.53	261.10		ice
20.00	1.50	11.3	253.54	260.99	276.73	$\text{NH}_4\text{HC}_2\text{O}_4\cdot 0.5\text{H}_2\text{O}$
20.00	2.00	8.5	253.47	266.68	285.81	$\text{NH}_4\text{HC}_2\text{O}_4\cdot 0.5\text{H}_2\text{O}$
20.00	3.00	5.7	253.50	261.08	293.24	$\text{NH}_4\text{HC}_2\text{O}_4\cdot 0.5\text{H}_2\text{O}$
20.00	4.00	4.2	253.49	261.28	297.45	$\text{NH}_4\text{HC}_2\text{O}_4\cdot 0.5\text{H}_2\text{O}$
20.00	5.00	3.4	253.45	266.49	313.66	
20.00	6.00	2.8	253.44	266.30	319.77	
20.00	7.00	2.4	253.45	266.05	325.19	$\text{NaHC}_2\text{O}_4\cdot\text{H}_2\text{O}$ <sup>b</sup>
30.00	1.00	25.4	253.52	261.44	267.70	$\text{NH}_4\text{HC}_2\text{O}_4\cdot 0.5\text{H}_2\text{O}$
30.00	1.50	17.0	253.47	261.32	280.87	$\text{NH}_4\text{HC}_2\text{O}_4\cdot 0.5\text{H}_2\text{O}$
30.00	2.00	12.7	253.47	261.27	292.60	$\text{NH}_4\text{HC}_2\text{O}_4\cdot 0.5\text{H}_2\text{O}$
30.00	3.00	8.5	253.51	261.14	301.11	$\text{NH}_4\text{HC}_2\text{O}_4\cdot 0.5\text{H}_2\text{O}$
30.00	4.00	6.4	253.51	260.95	307.01	$\text{NH}_4\text{HC}_2\text{O}_4\cdot 0.5\text{H}_2\text{O}$
30.00	5.00	5.1	253.45	260.68	310.32	$\text{NH}_4\text{HC}_2\text{O}_4\cdot 0.5\text{H}_2\text{O}$
30.00	5.50	4.6	253.46	260.04	311.21	$\text{NH}_4\text{HC}_2\text{O}_4\cdot 0.5\text{H}_2\text{O}$
30.00	6.00	4.2	253.36	260.40	323.23	$\text{NH}_4\text{HC}_2\text{O}_4\cdot 0.5\text{H}_2\text{O}$
30.00	7.00	3.6	253.43	260.38	330.18	$\text{NH}_4\text{HC}_2\text{O}_4\cdot 0.5\text{H}_2\text{O}$ <sup>b</sup>
40.00	1.01	33.6	251.69	255.61	273.65	$\text{NH}_4\text{HC}_2\text{O}_4\cdot 0.5\text{H}_2\text{O}$
40.00	1.50	22.6	251.55	255.44	288.47	$\text{NH}_4\text{HC}_2\text{O}_4\cdot 0.5\text{H}_2\text{O}$
40.00	2.00	17.0	251.46	255.38	291.55	$\text{NH}_4\text{HC}_2\text{O}_4\cdot 0.5\text{H}_2\text{O}$
40.01	2.50	13.6	253.46	261.47	306.91	$\text{NH}_4\text{HC}_2\text{O}_4\cdot 0.5\text{H}_2\text{O}$
40.00	3.00	11.3	253.49	263.7	321.24	$\text{NH}_4\text{HC}_2\text{O}_4\cdot 0.5\text{H}_2\text{O}$
40.00	4.00	8.5	253.45	276.45	328.96	$\text{NH}_4\text{HC}_2\text{O}_4\cdot 0.5\text{H}_2\text{O}$
40.00	5.00	6.8	253.47		331.42	$\text{NH}_4\text{HC}_2\text{O}_4\cdot 0.5\text{H}_2\text{O}$ <sup>b</sup>

<sup>a</sup>Concentrations are given in wt % and temperatures in Kelvin. <sup>b</sup>These samples were used for X-ray crystallographic analysis.

**Differential Scanning Calorimetry (DSC).** Thermal data were obtained with several Mettler Toledo DSC instruments: 822e and DSC1 with liquid nitrogen cooling and 822e and DSC1 cooled via an intra cooler. High-purity-grade nitrogen was used as a purge gas with a flow rate of 50 mL/min. The temperature reproducibility of these instruments is better than  $\pm 0.05$  K. Our accuracy is estimated to be  $\pm 0.9$  K with a probability of 0.94 based on a four-point temperature calibration<sup>25</sup> using indium, HPLC-grade water, anhydrous, high-purity (99%) octane, and anhydrous, high-purity heptane (99%) from Aldrich, the latter three stored under nitrogen. The enthalpy/heat capacity measurement of each DSC was also calibrated using the same substances and the known enthalpy of fusion for each substance, yielding an accuracy of  $\pm 3\%$  with a probability of 0.92.

Samples were contained in 40  $\mu\text{L}$  aluminum pans with crimped lids to create a seal and typically had a mass of approximately 15–25 mg. A typical sample was cooled to 183 at 10 K/min, held at that temperature for 5 min, and then warmed at a rate of 1 K/min to a temperature at least 5 K above the predicted dissolution point.

**Infrared Spectra.** The sample cell used for infrared spectra of liquid samples is similar to that described in previous literature.<sup>26</sup> A small drop of solution was placed between two ZnSe windows, which were held in the center of an aluminum block by a threaded metal ring. Sample volumes were

approximately 2  $\mu\text{L}$ . On each side of the aluminum block, a Pyrex cell was purged with dry nitrogen gas. KBr windows were placed on the end of each cell, sealed with o-rings, and held in place by metal clamps. The sample was cooled by pouring liquid nitrogen into a circular aluminum cup attached to the top of the main cell. The cell block was warmed by resistive heaters connected to a temperature controller. Temperature was measured by a copper/constantan thermocouple placed at the edge of the ZnSe windows and connected to the temperature controller. The temperature of the cell was calibrated using HPLC-grade water and high-purity organic solvents (Aldrich): decane, octane, and acetic anhydride, of which the melting points are 243.5, 216.4, and 200.2 K, respectively.<sup>27</sup> The IR cell temperatures are known on average to within  $\pm 1.3$  K, that is, a temperature that we measured in the IR cell of a specific transition is within 1.3 K of the transition temperature that we measure (of the same transition) using DSC. For solid samples, a Pike Technologies Miracle ATR accessory was used at room temperature (approximately 293 K).

Spectra were obtained with a Bruker Tensor 37 FTIR with a DTGS detector at 4  $\text{cm}^{-1}$  resolution. Each spectrum was the average of eight scans. Before spectra were taken of a sample, a background scan was obtained from a dry, purged sample cell (or an empty ATR cell for the solid samples). Liquid samples were cooled until the sample completely froze or to 200 K (whichever was a higher temperature) at 3 K/min and then

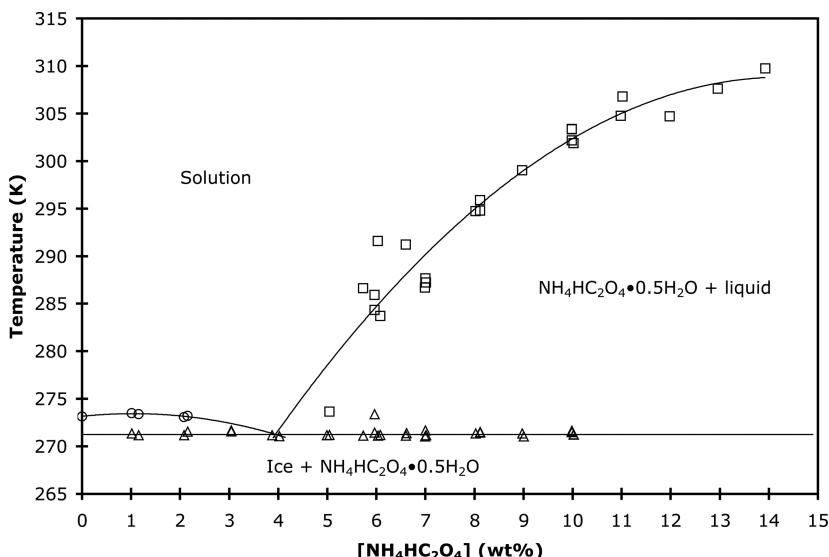


**Figure 1.** Partial phase diagram of the  $\text{NH}_4\text{HC}_2\text{O}_4/\text{H}_2\text{O}$  system: circles, ice melting; squares,  $\text{NH}_4\text{HC}_2\text{O}_4 \cdot 0.5\text{H}_2\text{O}$  dissolution; triangles, eutectic melting.

were allowed to warm to room temperature without resistive heating; typically this was 1 K/min or less. If the final target temperature was above room temperature, then resistive heating was applied to increase the temperature at about 1 K/min.

**X-ray Crystallography.** Crystal structures were determined at the Molecular Structure Laboratory in the Chemistry Department at the University of Wisconsin—Madison. Details of how these experiments are performed can be found in the Supporting Information of Kissinger et al.,<sup>24</sup> which is free of charge on the ACS Publications website at DOI: [10.1021/acs.jpca.6b02656](https://doi.org/10.1021/acs.jpca.6b02656).

## RESULTS

**NaHC<sub>2</sub>O<sub>4</sub>/H<sub>2</sub>O Binary System.** The solubility of  $\text{NaHC}_2\text{O}_4$  in water has been known for some time, and values appear in standard compilations,<sup>22</sup> with the precipitating crystal identified as  $\text{NaHC}_2\text{O}_4 \cdot \text{H}_2\text{O}$ . We were able to easily make saturated solutions of this compound by mixing NaOH and  $\text{H}_2\text{C}_2\text{O}_4$  in a 1:1 ratio at an elevated temperature (but below 323 K) and allowing the mixture to cool. A single crystal from a saturated solution was used for X-ray crystallographic analysis. The analysis confirmed that the salt present is  $\text{NaHC}_2\text{O}_4 \cdot \text{H}_2\text{O}$  by a match of the unit cell data with this compound in the Cambridge Crystallographic Database (CSD).<sup>28</sup> We also completely dried crystals from a saturated solution for IR analysis and found good agreement between our spectrum and that reported in the literature for  $\text{NaHC}_2\text{O}_4/\text{H}_2\text{O}$ <sup>29</sup> (see Figure S1 in the Supporting Information for an IR spectrum of our dried crystals). We ran DSC experiments on several concentrations of  $\text{NaHC}_2\text{O}_4$  in water to confirm the literature values. We found good agreement with literature values, as shown in the phase diagram plot of  $\text{NaHC}_2\text{O}_4/\text{H}_2\text{O}$  (Figure S2) in the Supporting Information. The ice/ $\text{NaHC}_2\text{O}_4 \cdot \text{H}_2\text{O}$  eutectic was determined to be 1.0 wt %  $\text{NaHC}_2\text{O}_4$  at a temperature of  $273.2 \pm 0.2$  K from an average of our values in DSC experiments.

**Na<sub>2</sub>C<sub>2</sub>O<sub>4</sub>/H<sub>2</sub>O Binary System.** The solubility of  $\text{Na}_2\text{C}_2\text{O}_4$  in water and ice melting temperatures have been known for some time, and values appear in standard compilations.<sup>22,23</sup> We

were able to easily make saturated solutions of this compound, and a single crystal from a saturated solution was used for X-ray crystallographic analysis. The analysis determined that the salt present is  $\text{Na}_2\text{C}_2\text{O}_4$  by a match of the unit cell data with this compound in the CSD.<sup>30</sup> We acquired an IR spectrum of crystals removed from a saturated solution that were subsequently dried before analysis and found good agreement with the NIST reference spectrum for  $\text{Na}_2\text{C}_2\text{O}_4$ <sup>31</sup> (see Figure S1 in the Supporting Information for our IR spectrum and the digitized NIST spectrum). We ran DSC experiments on several concentrations of  $\text{Na}_2\text{C}_2\text{O}_4$  in water to confirm the literature solubility values. We found good agreement with literature values, as shown in the phase diagram plot of  $\text{Na}_2\text{C}_2\text{O}_4/\text{H}_2\text{O}$  (Figure S3) in the Supporting Information. The eutectic transition for ice/ $\text{Na}_2\text{C}_2\text{O}_4$  was determined to be 2.6 wt %  $\text{Na}_2\text{C}_2\text{O}_4$  at a temperature of  $272.5 \pm 0.2$  K (average of DSC transitions.) The solubility of  $\text{Na}_2\text{C}_2\text{O}_4$  was also recently investigated by Rozaini and Brimblecomb;<sup>32</sup> however, their values are significantly higher than those reported in the literature and our DSC data (see Figure S4 in the Supporting Information.) Rozaini and Brimblecomb did not address this discrepancy, and we do not have an explanation for how they could obtain such high values for the solubility of sodium oxalate.

We also observed an endotherm in DSC experiments for all  $\text{Na}_2\text{C}_2\text{O}_4/\text{H}_2\text{O}$  samples at a temperature just below that of the eutectic, with an average value of  $270.9 \pm 0.2$  K. These transitions were small and had significant overlap with the eutectic transition. Our interpretation of this endothermic transition is that it likely represents the thermal decomposition of a hydrate of sodium oxalate, similar to that observed in the malonic acid/water system.<sup>33</sup> However, because of the low temperature of the transition and the small energy signal, we were not able to conclusively determine if this is a transition of a unique compound or identify the composition of this compound.

**NaHC<sub>2</sub>O<sub>4</sub>/(NH<sub>4</sub>)<sub>2</sub>SO<sub>4</sub>/H<sub>2</sub>O.** We explored the effect of ammonium sulfate on solutions of sodium hydrogen oxalate. Solutions were made by adding NaOH and  $\text{H}_2\text{C}_2\text{O}_4$  in a 1:1 ratio to aqueous solutions, which were also 10, 20, 30, or 40 wt

**Table 2.** Raw DSC Data for Endothermic Transitions in  $\text{NH}_4\text{HC}_2\text{O}_4/\text{H}_2\text{O}$  Samples<sup>a</sup>

[ $\text{NH}_4\text{HC}_2\text{O}_4$ ]	eutectic melt	final melt/dissolution
Ice Primary Phase Region		
0.00		273.15
1.01	271.38	273.48
1.15	271.18	273.4
2.08	271.17	273.08
2.15	271.54	273.19
3.04	271.68	
3.04	271.6	
3.87	271.19	
4.02	271.07	272.85
$\text{NH}_4\text{HC}_2\text{O}_4$ Primary Phase Region		
4.99	271.17	
5.04	271.2	273.66
5.73	271.15	286.63
5.96	273.39	285.94
5.96	271.45	284.34
6.03	271.14	291.61
6.08	271.21	283.7
6.60	271.15	291.22
6.61	271.39	
6.99	271.05	286.68
7.00	271.68	287.67
7.01	271.18	287.22
8.02	271.35	294.72
8.11	271.52	294.79
8.11	271.47	295.9
8.97	271.38	299.05
9.00	271.06	
9.98	271.5	302.16
9.98	271.58	303.35
9.98	271.66	303.37
10.02	271.24	301.88
10.02	271.28	
10.98	271.35	304.78
10.98	271.62	
11.02	271.41	306.8
11.02	271.61	
11.98	271.64	304.72
12.96	271.4	307.61
13.93	271.52	309.73

<sup>a</sup>Concentrations are given in wt % and temperatures in Kelvin.

% ( $\text{NH}_4$ )<sub>2</sub>SO<sub>4</sub>. Multiple crystallization and melting/dissolution transitions were observed in these samples in DSC and IR experiments; although, generally the typical melting pattern for a ternary system was observed: ternary eutectic melting, phase boundary melting, melt (dissolution) of the least soluble solid in its primary phase field. An example DSC thermogram is given in Figure S5 in the *Supporting Information* for a 10/6 wt % ( $\text{NH}_4$ )<sub>2</sub>SO<sub>4</sub>/NaHC<sub>2</sub>O<sub>4</sub> aqueous solution. In both DSC and IR experiments, the entire liquid phase tended to crystallize simultaneously, and thus, no glass transition was observed in our samples. Because of the low solubility of oxalate salts in this system, the IR spectra were dominated by ammonium and sulfate features; thus, transitions involving oxalate salts were not discernible in the IR experiments. However, it was generally clear in an IR spectrum when ice melted and ammonium sulfate dissolved into solution. Also, a consistent value for the ternary eutectic was observed in DSC experiments and confirmed with

IR experiments. We have correlated IR and DSC data for these transitions and report this raw data in *Table 1*. The average value of the ternary eutectic was found to be  $253.3 \pm 0.6$  K from DSC experiments.

To elucidate the identity of the last crystalline phase to be present upon warming before the sample converted to a completely liquid solution (highest-temperature endothermic transition in the DSC data), we utilized X-ray crystallography. To that end, we made solutions of the following concentrations: 10/7, 20/7, 30/7, 40/5 wt % ( $\text{NH}_4$ )<sub>2</sub>SO<sub>4</sub>/NaHC<sub>2</sub>O<sub>4</sub>. We chose these concentrations so that the solution would be saturated at room temperature, and a single crystal from each of these solutions was removed for X-ray crystallographic analysis. For each sample, the identity of the solid was determined by a match of the unit cell data with the compound in the CSD. For the 10 wt % ammonium sulfate sample, the least soluble solid was found to be  $\text{NaHC}_2\text{O}_4 \cdot \text{H}_2\text{O}$ .<sup>28</sup> For the 20 wt % ammonium sulfate sample, the solid was determined to be  $(\text{NaHC}_2\text{O}_4 \cdot \text{H}_2\text{O})_n$ ,<sup>34</sup> however, this appears to be a polymorph of  $\text{NaHC}_2\text{O}_4 \cdot \text{H}_2\text{O}$  and likely does not have a significantly different solubility. At high ammonium sulfate concentrations (30 and 40 wt %), the least soluble solid was found to be  $\text{NH}_4\text{HC}_2\text{O}_4 \cdot 0.5\text{H}_2\text{O}$  (ammonium hydrogen oxalate hemihydrate).<sup>35</sup> The mole ratio of ( $\text{NH}_4$ )<sub>2</sub>SO<sub>4</sub>/NaHC<sub>2</sub>O<sub>4</sub> for each of our samples is reported in *Table 1*. For the crystallographic analysis, samples where  $\text{NaHC}_2\text{O}_4 \cdot \text{H}_2\text{O}$  was the least soluble solid had ( $\text{NH}_4$ )<sub>2</sub>SO<sub>4</sub>/NaHC<sub>2</sub>O<sub>4</sub> mole ratios of 1.2 and 2.4, whereas samples where  $\text{NH}_4\text{HC}_2\text{O}_4 \cdot 0.5\text{H}_2\text{O}$  was the least soluble solid had ( $\text{NH}_4$ )<sub>2</sub>SO<sub>4</sub>/NaHC<sub>2</sub>O<sub>4</sub> mole ratios of 3.6 and 6.8. Thus, we can reasonably conclude that precipitation of  $\text{NH}_4\text{HC}_2\text{O}_4 \cdot 0.5\text{H}_2\text{O}$  in ternary solutions is favored at ( $\text{NH}_4$ )<sub>2</sub>SO<sub>4</sub>/NaHC<sub>2</sub>O<sub>4</sub> mole ratios  $\geq 3.6$ , while the precipitation of  $\text{NaHC}_2\text{O}_4 \cdot \text{H}_2\text{O}$  is favored at ( $\text{NH}_4$ )<sub>2</sub>SO<sub>4</sub>/NaHC<sub>2</sub>O<sub>4</sub> mole ratios  $\leq 2.4$ . Hence, we have assigned the likely least soluble salt present in our samples as given in *Table 1* based on this observation and left identity of the precipitate in the ( $\text{NH}_4$ )<sub>2</sub>SO<sub>4</sub>/NaHC<sub>2</sub>O<sub>4</sub> mole ratio range of 2.4–3.6 uncertain.

The solubility of  $\text{NH}_4\text{HC}_2\text{O}_4 \cdot 0.5\text{H}_2\text{O}$  in water has not been reported in the literature to our knowledge, and thus, we undertook the measurement of solubilities in the  $\text{NH}_4\text{HC}_2\text{O}_4/\text{H}_2\text{O}$  system for comparison with our ternary samples. Solutions were made by mixing  $\text{NH}_4\text{OH}$  with  $\text{H}_2\text{C}_2\text{O}_4$  in a 1:1 mole ratio in water. The results of DSC experiments are given in *Figure 1*, showing a partial phase diagram of the water/ $\text{NH}_4\text{HC}_2\text{O}_4$  system with the raw data given in *Table 2*. An example DSC thermogram for a 12 wt %  $\text{NH}_4\text{HC}_2\text{O}_4$  aqueous solution is given in Figure S5 in the *Supporting Information*. X-ray crystallography of crystals from a solution saturated at room temperature confirmed the solid to be  $\text{NH}_4\text{HC}_2\text{O}_4 \cdot 0.5\text{H}_2\text{O}$ .<sup>36</sup> The scatter in the solubility data for  $\text{NH}_4\text{HC}_2\text{O}_4 \cdot 0.5\text{H}_2\text{O}$  in *Figure 1* is due to the small concentrations and very small enthalpy of dissolution for this salt, thus leading to greater uncertainty in the final dissolution temperatures of the salt. Nonetheless, the general trend is clear and can be used for comparison with other solubilities.

We have plotted the solubilities that we measured in the  $\text{NaHC}_2\text{O}_4/(\text{NH}_4)_2\text{SO}_4/\text{H}_2\text{O}$  system in *Figure 2* (data from *Table 1*) for 10, 20, 30, and 40 wt % ammonium sulfate solutions along with the solubility of  $\text{NaHC}_2\text{O}_4 \cdot \text{H}_2\text{O}$  from Linke<sup>22</sup> and our values for  $\text{NH}_4\text{HC}_2\text{O}_4 \cdot 0.5\text{H}_2\text{O}$ . In the solutions where  $\text{NaHC}_2\text{O}_4 \cdot \text{H}_2\text{O}$  formed (10 and 20 wt % ( $\text{NH}_4$ )<sub>2</sub>SO<sub>4</sub>), it is seen that ammonium sulfate has a “salting in” effect on  $\text{NaHC}_2\text{O}_4 \cdot \text{H}_2\text{O}$ , that is,  $\text{NaHC}_2\text{O}_4 \cdot \text{H}_2\text{O}$  is more

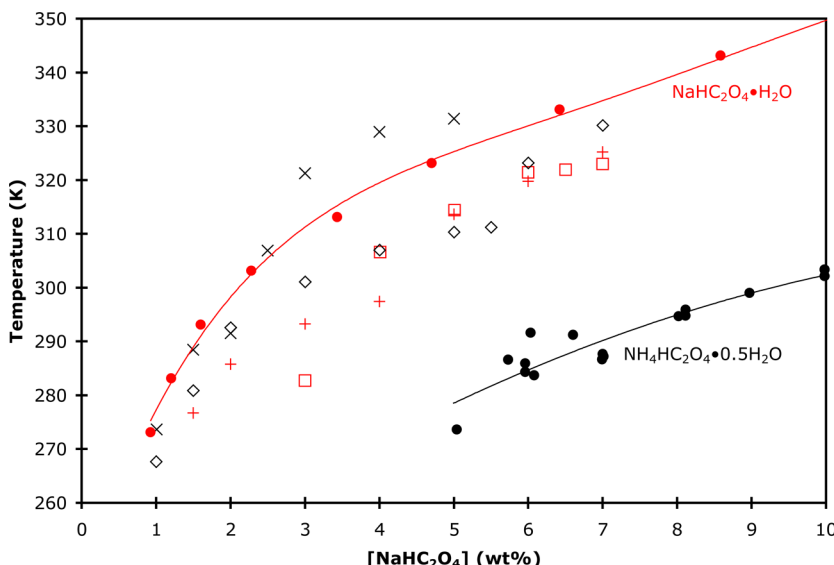


**Figure 2.** Solubilities of solids in the  $(\text{NH}_4)_2\text{SO}_4/\text{NaHC}_2\text{O}_4/\text{H}_2\text{O}$  system. Red symbols are where  $\text{NaHC}_2\text{O}_4 \cdot \text{H}_2\text{O}$  is the least soluble solid, and black symbols are where  $\text{NH}_4\text{HC}_2\text{O}_4 \cdot 0.5\text{H}_2\text{O}$  is the least soluble solid. Solid black symbols represent the solubility of  $\text{NH}_4\text{HC}_2\text{O}_4 \cdot 0.5\text{H}_2\text{O}$  in aqueous solutions of 1:1  $\text{NH}_4\text{OH}/\text{H}_2\text{C}_2\text{O}_4$  from our experiments. Solid red symbols represent the solubility of  $\text{NaHC}_2\text{O}_4 \cdot \text{H}_2\text{O}$  in water from Linke.<sup>22</sup> Other symbols are our measurements for  $\text{NaHC}_2\text{O}_4$  in water with 10 wt %  $(\text{NH}_4)_2\text{SO}_4$ , squares; 20 wt %  $(\text{NH}_4)_2\text{SO}_4$ , crosses; 30 wt %  $(\text{NH}_4)_2\text{SO}_4$ , diamonds; 40 wt %  $(\text{NH}_4)_2\text{SO}_4$ , exes.

soluble in water in the presence of  $(\text{NH}_4)_2\text{SO}_4$  than that without it. However, for the solutions where  $\text{NH}_4\text{HC}_2\text{O}_4 \cdot 0.5\text{H}_2\text{O}$  forms (30 and 40 wt %  $(\text{NH}_4)_2\text{SO}_4$ , where there is a high concentration of ammonium ions), the presence of ammonium sulfate has a “salting out” effect on  $\text{NH}_4\text{HC}_2\text{O}_4 \cdot 0.5\text{H}_2\text{O}$ , that is,  $\text{NH}_4\text{HC}_2\text{O}_4 \cdot 0.5\text{H}_2\text{O}$  is less soluble in water where  $(\text{NH}_4)_2\text{SO}_4$  is also present. Whichever solid forms, its solubility is relatively independent of ammonium sulfate concentration, except for samples that were 40 wt %  $(\text{NH}_4)_2\text{SO}_4$  and  $[\text{NaHC}_2\text{O}_4] > 2$  wt %. Here,  $\text{NH}_4\text{HC}_2\text{O}_4 \cdot 0.5\text{H}_2\text{O}$  was less soluble than that in solutions that were 30 wt %  $(\text{NH}_4)_2\text{SO}_4$  and had similar concentrations of  $\text{NaHC}_2\text{O}_4$ . Thus, this system appears complex, and the solids that may precipitate clearly depend on the ammonium concentration. It is apparent that high ammonium concentration shifts the probability of solid formation toward  $\text{NH}_4\text{HC}_2\text{O}_4 \cdot 0.5\text{H}_2\text{O}$  even though it is more soluble than  $\text{NaHC}_2\text{O}_4 \cdot \text{H}_2\text{O}$  in water, yet the solubility of  $\text{NH}_4\text{HC}_2\text{O}_4 \cdot 0.5\text{H}_2\text{O}$  in the presence of excess  $\text{NH}_4^+$  and  $\text{SO}_4^{2-}$  ions is comparable or lower than that of  $\text{NaHC}_2\text{O}_4 \cdot \text{H}_2\text{O}$  under the same conditions.

**$\text{Na}_2\text{C}_2\text{O}_4/(\text{NH}_4)_2\text{SO}_4/\text{H}_2\text{O}$ .** We explored the effect of ammonium sulfate on aqueous solutions of sodium oxalate. Solutions were made by adding  $\text{NaOH}$  and  $\text{H}_2\text{C}_2\text{O}_4$  in a 2:1 ratio to aqueous solutions, which were also 5, 10, 20, 30, or 40 wt %  $(\text{NH}_4)_2\text{SO}_4$ . Multiple crystallization and melting/dissolution transitions were observed in these samples in DSC and IR experiments, although the typical melting pattern for a ternary system was generally observed: ternary eutectic melting, phase boundary melting, melt/dissolution of the least soluble solid in its primary phase field. An example DSC thermogram is given in Figure S5 in the *Supporting Information* for a 20/5 wt %  $(\text{NH}_4)_2\text{SO}_4/\text{Na}_2\text{C}_2\text{O}_4$  aqueous solution. In both DSC and IR experiments, the entire liquid phase tended to crystallize simultaneously, and thus, no glass transitions were observed. Because of the complexity of these solutions and overlapping IR absorption bands, it again was not possible to uniquely identify all phases present at any given

temperature from the IR and DSC data alone. However, it is generally clear in an IR spectrum when ice melts, and a consistent value for the ternary eutectic was observed in DSC experiments and confirmed with IR experiments. We have correlated the IR and DSC data for ice melting and report this raw data in Table 3 along with the ternary eutectic and final melt/dissolution temperatures. The average value of the ternary eutectic was found to be  $253.4 \pm 0.5$  K from DSC experiments.

To elucidate the identity of the last crystalline phase present upon warming before the sample is converted to a completely liquid solution (highest-temperature endothermic transition in the DSC data), we utilized X-ray crystallography. To that end, we made saturated solutions of the following concentrations: 5/6, 10/6, 20/3, 20/6, 30/2, 40/1 wt %  $(\text{NH}_4)_2\text{SO}_4/\text{Na}_2\text{C}_2\text{O}_4$ . A single crystal from each of these solutions was removed at room temperature for X-ray crystallographic analysis. For samples of 10, 20, 30, and 40 wt %  $(\text{NH}_4)_2\text{SO}_4$ , the solid was identified as  $(\text{NH}_4)_2\text{C}_2\text{O}_4 \cdot \text{H}_2\text{O}$  (ammonium oxalate monohydrate) by a match of the unit cell data with this compound in the CSD.<sup>37</sup> The solubility of this compound in water is available in standard compilations<sup>22,23</sup> but is based on the work of Hill and Distler.<sup>38</sup> The  $(\text{NH}_4)_2\text{SO}_4/\text{Na}_2\text{C}_2\text{O}_4$  mole ratio of our samples is given in Table 2, and for  $[(\text{NH}_4)_2\text{SO}_4] \geq 10$  wt %, the  $(\text{NH}_4)_2\text{SO}_4/\text{Na}_2\text{C}_2\text{O}_4$  mole ratio is  $\geq 1.7$ . In contrast, the least soluble solid in the 5/6 wt %  $(\text{NH}_4)_2\text{SO}_4/\text{Na}_2\text{C}_2\text{O}_4$  sample was found to be  $\text{Na}_2\text{C}_2\text{O}_4$  by a match of the unit cell data with this compound in the CSD.<sup>39</sup> This sample has an  $(\text{NH}_4)_2\text{SO}_4/\text{Na}_2\text{C}_2\text{O}_4$  mole ratio equal to 0.8. Thus, we conclude that  $\text{Na}_2\text{C}_2\text{O}_4$  is the least soluble solid in ternary samples for  $(\text{NH}_4)_2\text{SO}_4/\text{Na}_2\text{C}_2\text{O}_4$  mole ratios  $\leq 0.8$ , while  $(\text{NH}_4)_2\text{C}_2\text{O}_4 \cdot \text{H}_2\text{O}$  is the least soluble solid for  $(\text{NH}_4)_2\text{SO}_4/\text{Na}_2\text{C}_2\text{O}_4$  mole ratios  $\geq 1.7$ . We have used this criteria to identify the least soluble solid for all of our samples, as given in Table 3.

We have plotted the solubilities that we measured in Figure 3 along with the solubility of ammonium oxalate monohydrate from Hill and Distler<sup>38</sup> and the solubility of  $\text{Na}_2\text{C}_2\text{O}_4$  from Stephen et al.<sup>23</sup> In general, we observe that at  $[(\text{NH}_4)_2\text{SO}_4] \geq$

Table 3. Raw DSC and IR Data for Endothermic Transitions in  $(\text{NH}_4)_2\text{SO}_4/\text{Na}_2\text{C}_2\text{O}_4$  Samples<sup>a</sup>

$[(\text{NH}_4)_2\text{SO}_4]$	$[\text{Na}_2\text{C}_2\text{O}_4]$	mole ratio $(\text{NH}_4)_2\text{SO}_4/\text{Na}_2\text{C}_2\text{O}_4$	ternary eutectic	ice melt	final salt dissolution	identity of final melting/dissolving compound
5.00	2.96	1.7	250.02	272.35	282.3	$(\text{NH}_4)_2\text{C}_2\text{O}_4 \cdot \text{H}_2\text{O}$
5.03	4.49	1.1	252.6	272.06	286.5	$\text{Na}_2\text{C}_2\text{O}_4^c$
4.99	6.03	0.8	270.71		290.84	$\text{Na}_2\text{C}_2\text{O}_4^b$
10.00	0.50	20.3	253.53	270.55		ice
10.00	1.00	10.1	253.6	270.61	283.81	$(\text{NH}_4)_2\text{C}_2\text{O}_4 \cdot \text{H}_2\text{O}$
10.00	1.50	6.8	253.56	270.71	289.31	$(\text{NH}_4)_2\text{C}_2\text{O}_4 \cdot \text{H}_2\text{O}$
10.00	2.00	5.1	253.57	270.76	293.41	$(\text{NH}_4)_2\text{C}_2\text{O}_4 \cdot \text{H}_2\text{O}$
10.00	3.01	3.4	253.55	270.76	299.32	$(\text{NH}_4)_2\text{C}_2\text{O}_4 \cdot \text{H}_2\text{O}$
10.00	3.00	3.4	253.72	270.76	298.29	$(\text{NH}_4)_2\text{C}_2\text{O}_4 \cdot \text{H}_2\text{O}$
10.00	4.00	2.5	253.58	270.90	308.26	$(\text{NH}_4)_2\text{C}_2\text{O}_4 \cdot \text{H}_2\text{O}$
10.00	5.00	2.0	253.49	270.9	309.64	$(\text{NH}_4)_2\text{C}_2\text{O}_4 \cdot \text{H}_2\text{O}$
10.01	6.01	1.7	253.41	271.21	312.73	$(\text{NH}_4)_2\text{C}_2\text{O}_4 \cdot \text{H}_2\text{O}^b$
20.01	0.51	39.8	253.46	267.11		ice
20.00	1.00	20.3	253.52	267.00		ice
20.00	1.25	16.2	253.80	267.36	298.16	$(\text{NH}_4)_2\text{C}_2\text{O}_4 \cdot \text{H}_2\text{O}$
20.00	1.50	13.5	253.76	267.14	302.95	$(\text{NH}_4)_2\text{C}_2\text{O}_4 \cdot \text{H}_2\text{O}$
20.00	2.00	10.1	253.53	266.88	304.13	$(\text{NH}_4)_2\text{C}_2\text{O}_4 \cdot \text{H}_2\text{O}$
20.00	2.00	10.1	253.73	267.09	308.79	$(\text{NH}_4)_2\text{C}_2\text{O}_4 \cdot \text{H}_2\text{O}$
20.00	3.01	6.7	250.89	266.29	310.59	$(\text{NH}_4)_2\text{C}_2\text{O}_4 \cdot \text{H}_2\text{O}^b$
20.00	4.00	5.1	253.41	267.12	313.56	$(\text{NH}_4)_2\text{C}_2\text{O}_4 \cdot \text{H}_2\text{O}$
20.00	5.00	4.1	253.52	267.00	319.56	$(\text{NH}_4)_2\text{C}_2\text{O}_4 \cdot \text{H}_2\text{O}$
20.00	6.00	3.4	253.53	267.05	323.84	$(\text{NH}_4)_2\text{C}_2\text{O}_4 \cdot \text{H}_2\text{O}^b$
30.00	0.50	60.8	253.46	261.66		ice
30.00	1.00	30.4	253.53	261.60		ice
30.00	1.50	20.3	253.71	261.88	313.43	$(\text{NH}_4)_2\text{C}_2\text{O}_4 \cdot \text{H}_2\text{O}$
30.00	2.00	15.2	253.46	261.09	325.83	$(\text{NH}_4)_2\text{C}_2\text{O}_4 \cdot \text{H}_2\text{O}^b$
30.00	3.00	10.1	253.38	261.03	328.77	$(\text{NH}_4)_2\text{C}_2\text{O}_4 \cdot \text{H}_2\text{O}$
30.00	4.00	7.6	253.43	261.11	330.81	$(\text{NH}_4)_2\text{C}_2\text{O}_4 \cdot \text{H}_2\text{O}$
40.00	0.25	162.3	253.08	258.69		ice
40.00	0.50	81.1	253.06	255.99		ice
40.00	1.00	40.6	252.95	255.57	324	$(\text{NH}_4)_2\text{C}_2\text{O}_4 \cdot \text{H}_2\text{O}^b$
39.99	1.50	27.0	253.37	255.57	329.67	$(\text{NH}_4)_2\text{C}_2\text{O}_4 \cdot \text{H}_2\text{O}$
39.99	2.00	20.3	253.73		331.27	$(\text{NH}_4)_2\text{C}_2\text{O}_4 \cdot \text{H}_2\text{O}$

<sup>a</sup>Concentrations are given in wt % and temperatures in Kelvin. <sup>b</sup>These samples were used for X-ray crystallographic analysis. <sup>c</sup>Identity assigned as described in the text.

10 wt %,  $(\text{NH}_4)_2\text{C}_2\text{O}_4 \cdot \text{H}_2\text{O}$  is the least soluble solid, and an increasing salting out effect on ammonium oxalate monohydrate with increasing ammonium sulfate concentration is observed; as the  $(\text{NH}_4)_2\text{SO}_4$  concentration increases,  $(\text{NH}_4)_2\text{C}_2\text{O}_4 \cdot \text{H}_2\text{O}$  becomes less soluble. The solubility of sodium oxalate appears more complicated. We note that sodium oxalate solubility has a much stronger temperature dependence (solid red circles and red line in Figure 3) than does ammonium oxalate monohydrate with and without ammonium sulfate present. What is unexpected is that solutions with a concentration of  $\text{Na}_2\text{C}_2\text{O}_4$  greater than the solubility limit of  $\text{Na}_2\text{C}_2\text{O}_4$  in water were found to form  $(\text{NH}_4)_2\text{C}_2\text{O}_4 \cdot \text{H}_2\text{O}$  from a solution with  $(\text{NH}_4)_2\text{SO}_4$  present (10 and 20 wt %  $(\text{NH}_4)_2\text{SO}_4$  solutions with  $[\text{Na}_2\text{C}_2\text{O}_4] \geq 4$  wt %). The explanation for this observation comes from our experiments at 5 wt %  $(\text{NH}_4)_2\text{SO}_4$  where we observed  $\text{Na}_2\text{C}_2\text{O}_4$  to be the least soluble solid for 5/6 wt %  $(\text{NH}_4)_2\text{SO}_4/\text{Na}_2\text{C}_2\text{O}_4$ , and its solubility in the presence of ammonium sulfate is greater than that in water without ammonium sulfate present (red squares in Figure 3). While we do not have X-ray crystallographic data for the 5/4.5 wt %  $(\text{NH}_4)_2\text{SO}_4/\text{Na}_2\text{C}_2\text{O}_4$  sample, the final dissolution temperature for the solid in this sample is below that of  $\text{Na}_2\text{C}_2\text{O}_4$  and  $(\text{NH}_4)_2\text{C}_2\text{O}_4 \cdot \text{H}_2\text{O}$  in water. Because ammonium sulfate appears to only have a salting out effect on

$(\text{NH}_4)_2\text{C}_2\text{O}_4 \cdot \text{H}_2\text{O}$ , it is reasonable to conclude that the solid present in our 5/4.5 wt % sample is  $\text{Na}_2\text{C}_2\text{O}_4$ , as indicated by using a red square for the solubility of this sample in Figure 3. The  $(\text{NH}_4)_2\text{SO}_4/\text{Na}_2\text{C}_2\text{O}_4$  mole ratio in this sample is 1.1 and thus extends the limit for  $\text{Na}_2\text{C}_2\text{O}_4$  formation in this ternary system. However, for our 5/3 wt %  $(\text{NH}_4)_2\text{SO}_4/\text{Na}_2\text{C}_2\text{O}_4$  sample where the  $(\text{NH}_4)_2\text{SO}_4/\text{Na}_2\text{C}_2\text{O}_4$  mole ratio is 1.7, the least soluble solid should be  $(\text{NH}_4)_2\text{C}_2\text{O}_4 \cdot \text{H}_2\text{O}$ , as predicted by our observations described above. This prediction is in line with the solubility that we observe, which falls on or is slightly less than the  $(\text{NH}_4)_2\text{C}_2\text{O}_4 \cdot \text{H}_2\text{O}/\text{H}_2\text{O}$  solubility data and best-fit curve (black curve in Figure 3); we have indicated this point by a black square in Figure 3. In summary, in addition to having a salting out effect on  $(\text{NH}_4)_2\text{C}_2\text{O}_4 \cdot \text{H}_2\text{O}$ , ammonium sulfate has a salting in effect on  $\text{Na}_2\text{C}_2\text{O}_4$ . This is analogous to what we observed in the  $\text{NaHC}_2\text{O}_4/(\text{NH}_4)_2\text{SO}_4/\text{H}_2\text{O}$  samples, though the transition between the two regimes occurs at much lower mole ratios of ammonium sulfate to oxalate.

## DISCUSSION AND ATMOSPHERIC IMPLICATIONS

In atmospheric droplets that contain oxalic acid, ammonium, sulfate, and sodium ions, several salts can form that are less soluble than either ammonium sulfate or oxalic acid dihydrate. Table 4 gives a summary of the identity of the least soluble

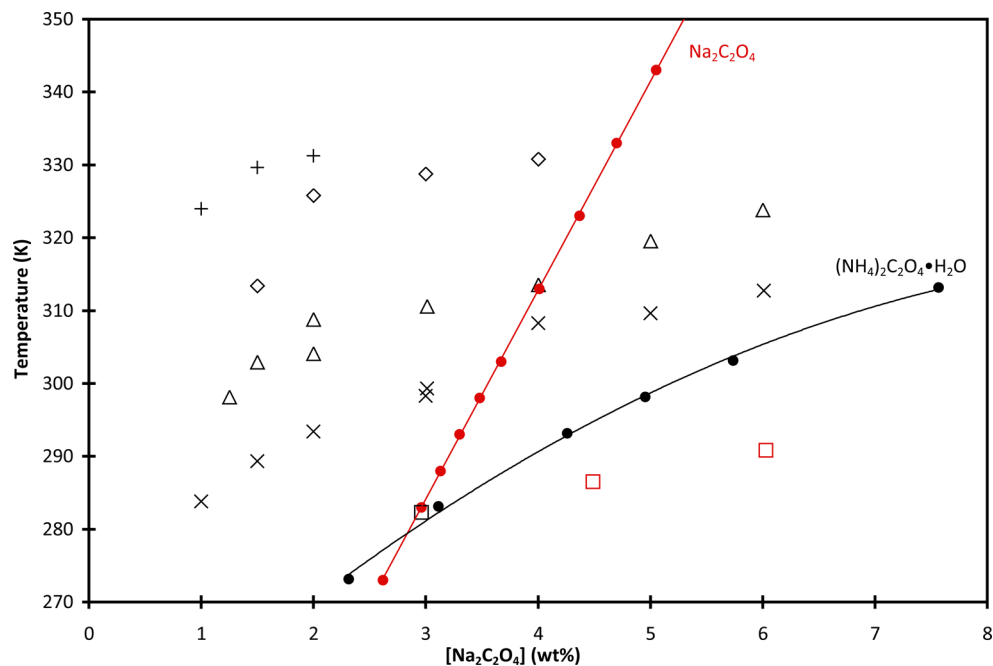
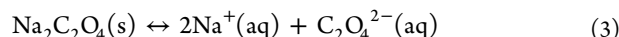
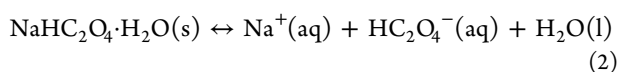


**Figure 3.** Solubilities of solids in the  $(\text{NH}_4)_2\text{SO}_4/\text{Na}_2\text{C}_2\text{O}_4/\text{H}_2\text{O}$  system. Red symbols are where  $\text{Na}_2\text{C}_2\text{O}_4$  is the least soluble solid, and black symbols are where  $(\text{NH}_4)_2\text{C}_2\text{O}_4\cdot\text{H}_2\text{O}$  is the least soluble solid. Solid black symbols represent the solubility of  $(\text{NH}_4)_2\text{C}_2\text{O}_4\cdot\text{H}_2\text{O}$  in water from Hill and Distler.<sup>38</sup> Solid red symbols represent the solubility of  $\text{Na}_2\text{C}_2\text{O}_4$  in water from Stephen et al.<sup>23</sup> Other symbols are from our experiments of  $\text{Na}_2\text{C}_2\text{O}_4$  in water with 5 wt %  $(\text{NH}_4)_2\text{SO}_4$ , squares; 10 wt %  $(\text{NH}_4)_2\text{SO}_4$ , exes; 20 wt %  $(\text{NH}_4)_2\text{SO}_4$ , triangles; 30 wt %  $(\text{NH}_4)_2\text{SO}_4$ , diamonds; 40 wt %  $(\text{NH}_4)_2\text{SO}_4$ , crosses.

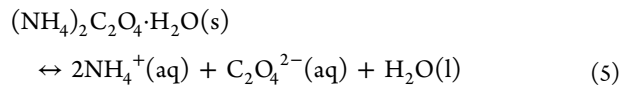
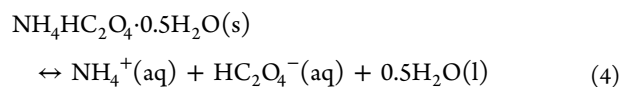
**Table 4. Summary of the Least Soluble Compounds in Aqueous  $\text{NaHC}_2\text{O}_4$  and  $\text{Na}_2\text{C}_2\text{O}_4$  Systems with and without  $(\text{NH}_4)_2\text{SO}_4$**

organic salt	inorganic salt	$(\text{NH}_4)_2\text{SO}_4/\text{oxalate}$ mole ratio	least soluble solid
$\text{NaHC}_2\text{O}_4$	$(\text{NH}_4)_2\text{SO}_4$	$\leq 2.4$	$\text{NaHC}_2\text{O}_4\cdot\text{H}_2\text{O}$
		$\geq 3.6$	$\text{NaHC}_2\text{O}_4\cdot\text{H}_2\text{O}$ $\text{NH}_4\text{HC}_2\text{O}_4\cdot 0.5\text{H}_2\text{O}$
$\text{Na}_2\text{C}_2\text{O}_4$	$(\text{NH}_4)_2\text{SO}_4$	$\leq 1.1$	$\text{Na}_2\text{C}_2\text{O}_4$
		$\geq 1.7$	$\text{Na}_2\text{C}_2\text{O}_4$ $(\text{NH}_4)_2\text{C}_2\text{O}_4\cdot\text{H}_2\text{O}$

solids in solutions of varying concentrations of each salt. The effects of ammonium sulfate on the solubility of organic salts are generally not accounted for in atmospheric aerosol models because they are based on/constrained by experimental data,<sup>40–42</sup> and there is little data in the literature involving solubility in aqueous organic and inorganic salt mixtures. However, it is clear from our experimental results that ammonium sulfate has a significant impact on the solubility of the sodium and ammonium salts of oxalic acid. Thus, in areas of high ammonium sulfate content, the oxalate ions present may precipitate in aqueous aerosols as one of the ammonium oxalate salts before ammonium sulfate or any of the sodium salts reach saturation. In fact, only under conditions of low ammonium sulfate concentration in aerosols will the sodium salts of oxalic acid precipitate. Even though ammonium sulfate does not generate an ion in common with the sodium oxalate salts in solution



ammonium sulfate does exhibit a salting in effect on both  $\text{NaHC}_2\text{O}_4\cdot\text{H}_2\text{O}$  and  $\text{Na}_2\text{C}_2\text{O}_4$ . The most probable explanation for this effect is that the ammonium ions from  $(\text{NH}_4)_2\text{SO}_4$  stabilize the  $\text{HC}_2\text{O}_4^-$  and  $\text{C}_2\text{O}_4^{2-}$  species in solution, thus allowing a greater solubility of the oxalate salts. In the case of the ammonium oxalates, there is a common ion with ammonium sulfate in solution



and therefore the salting out effect of  $(\text{NH}_4)_2\text{SO}_4$  on the ammonium oxalates can be contributed to the shift in the solubility equilibrium due to increased ammonium concentration. This is seen most clearly in Figure 3 where the  $(\text{NH}_4)_2\text{C}_2\text{O}_4\cdot\text{H}_2\text{O}$  solubility decreases as the  $(\text{NH}_4)_2\text{SO}_4$  concentration increases. The effect is similar, though less pronounced, for  $\text{NH}_4\text{HC}_2\text{O}_4\cdot 0.5\text{H}_2\text{O}$ , as seen in Figure 2.

We present a summary of the solubilities of various salts in Figure 4 as a function of mole fraction salt so that solubilities can be compared on a mole basis. It is seen that ammonium sulfate is by far the most soluble salt of those compared. Sodium sulfate decahydrate is the next most soluble at temperatures above 283 K where the  $\text{Na}_2\text{SO}_4\cdot 10\text{H}_2\text{O}$  solubility crosses the solubility of oxalic acid dihydrate (at higher temperatures,  $\text{Na}_2\text{SO}_4$  becomes less soluble than  $\text{H}_2\text{C}_2\text{O}_4\cdot 2\text{H}_2\text{O}$ ). Ammonium hydrogen oxalate hemihydrate is the next most soluble salt; however, this is in the absence of ammonium sulfate. As we described above, ammonium sulfate has a salting

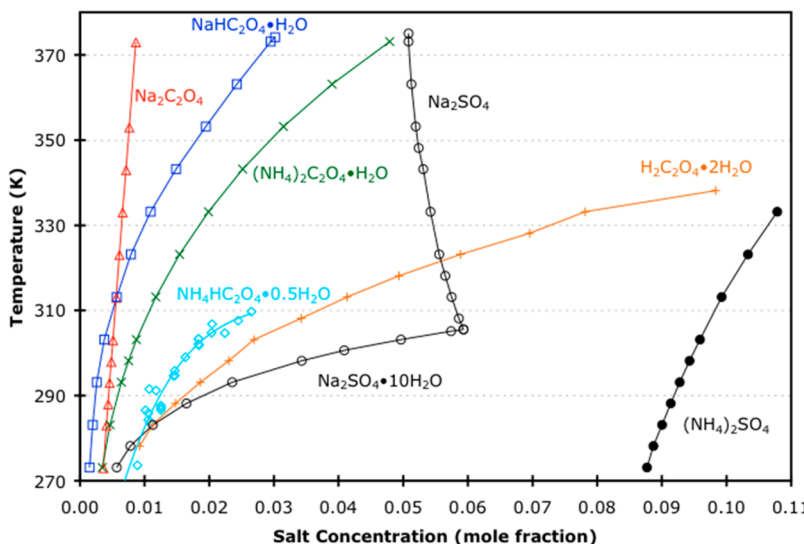


**Figure 4.** Summary of salt solubilities as a function of the mole fraction of the solute in water. Data for  $\text{Na}_2\text{SO}_4 \cdot 10\text{H}_2\text{O}$  and  $\text{Na}_2\text{SO}_4$  (black circles),  $\text{NaHC}_2\text{O}_4 \cdot \text{H}_2\text{O}$  (blue squares), and  $(\text{NH}_4)_2\text{C}_2\text{O}_4 \cdot \text{H}_2\text{O}$  (green exes) are from Linke.<sup>22</sup> Data for  $(\text{NH}_4)_2\text{SO}_4$  (solid black circles) and  $\text{Na}_2\text{C}_2\text{O}_4$  (red triangles) are from Stephen et al.<sup>23</sup> Data for  $\text{H}_2\text{C}_2\text{O}_4 \cdot 2\text{H}_2\text{O}$  (orange crosses) are from Apelblat and Manzurola.<sup>43</sup> Data for  $\text{NH}_4\text{HC}_2\text{O}_4 \cdot 0.5\text{H}_2\text{O}$  (light blue diamonds) are from this study. Lines connecting points are present to aid in seeing the trend in solubility for each salt and are not fits to the data.

out effect on  $\text{NH}_4\text{HC}_2\text{O}_4 \cdot 0.5\text{H}_2\text{O}$ , and in fact, at moderate to high ammonium sulfate concentrations,  $\text{NH}_4\text{HC}_2\text{O}_4 \cdot 0.5\text{H}_2\text{O}$  solubility becomes roughly equal to that of sodium hydrogen oxalate monohydrate in water (blue squares in Figure 4). Thus, at tropospheric temperatures in the presence of ammonium sulfate,  $\text{NH}_4\text{HC}_2\text{O}_4 \cdot 0.5\text{H}_2\text{O}$  becomes one of the least soluble salts that can be present in this mixture. However, because of the strong salting out effect of ammonium sulfate on  $(\text{NH}_4)_2\text{C}_2\text{O}_4 \cdot \text{H}_2\text{O}$ , it becomes even less soluble at tropospheric temperatures and moderate to high ammonium sulfate concentration. These observations are the opposite of what one would expect to occur in atmospheric aerosols if the solubilities of the various salts in water were exclusively considered (absent in the presence of ammonium sulfate). Without ammonium sulfate, the sodium oxalates would be expected to be the least soluble salts in water, as shown in Figure 4. Because the presence of ammonium sulfate has a significant salting out effect on the ammonium oxalates, making them less soluble than the sodium oxalates, their formation must be considered when modeling the atmospheric aerosol composition and in explaining field observations where chemical composition is an important consideration.

## SUMMARY

We have measured the solubility of sodium hydrogen oxalate and sodium oxalate in aqueous solutions of varying concentrations of ammonium sulfate. For both organic salts, the identity of the least soluble salt was found to be a function of the ratio of ammonium sulfate to oxalate in solution. At low ammonium sulfate to oxalate ratios, the least soluble salts were  $\text{NaHC}_2\text{O}_4 \cdot \text{H}_2\text{O}$  and  $\text{Na}_2\text{C}_2\text{O}_4$ . At high ammonium sulfate to oxalate ratios, the least soluble salts were found to be  $\text{NH}_4\text{HC}_2\text{O}_4 \cdot 0.5\text{H}_2\text{O}$  and  $(\text{NH}_4)_2\text{C}_2\text{O}_4 \cdot \text{H}_2\text{O}$ . The solubility of  $\text{NH}_4\text{HC}_2\text{O}_4 \cdot 0.5\text{H}_2\text{O}$  had not previously been known, and we determined a partial phase diagram for the  $\text{NH}_4\text{HC}_2\text{O}_4 \cdot 0.5\text{H}_2\text{O}/\text{H}_2\text{O}$  system. In both ternary systems, ammonium sulfate had the effect of salting in  $\text{NaHC}_2\text{O}_4 \cdot \text{H}_2\text{O}$  and  $\text{Na}_2\text{C}_2\text{O}_4$  and salting out  $\text{NH}_4\text{HC}_2\text{O}_4 \cdot 0.5\text{H}_2\text{O}$  and  $(\text{NH}_4)_2\text{C}_2\text{O}_4 \cdot \text{H}_2\text{O}$ .

when compared to their respective solubilities in water without ammonium sulfate present. The result is that the ammonium oxalate salts are less soluble than the other compounds that could precipitate from these ternary solutions at tropospheric temperatures under moderate to high ammonium sulfate concentrations:  $(\text{NH}_4)_2\text{SO}_4$ ,  $\text{Na}_2\text{SO}_4$ ,  $\text{Na}_2\text{SO}_4 \cdot 10\text{H}_2\text{O}$ ,  $\text{H}_2\text{C}_2\text{O}_4 \cdot 2\text{H}_2\text{O}$ , or  $\text{NaNH}_4\text{SO}_4 \cdot 2\text{H}_2\text{O}$ .<sup>24</sup> Under low ammonium sulfate conditions, the sodium oxalate salts are more soluble in aqueous solution than when ammonium sulfate is absent. These results have implications for which salts are predicted to form in tropospheric aerosols where sodium, ammonium, oxalate, hydrogen oxalate and sulfate are present.

## ASSOCIATED CONTENT

### Supporting Information

The Supporting Information is available free of charge on the ACS Publications website at DOI: 10.1021/acs.jpca.6b05208.

Infrared spectra for  $\text{NaHC}_2\text{O}_4 \cdot \text{H}_2\text{O}$  and  $\text{Na}_2\text{C}_2\text{O}_4$ ; a partial phase diagrams for  $\text{NaHC}_2\text{O}_4/\text{H}_2\text{O}$  and  $\text{Na}_2\text{C}_2\text{O}_4/\text{H}_2\text{O}$  from literature and our DSC data,  $\text{Na}_2\text{C}_2\text{O}_4$  solubility data from Rozaini and Brimblecomb with other literature data and our DSC data, and DSC thermograms of the warming segment for aqueous solutions of  $(\text{NH}_4)_2\text{SO}_4/\text{NaHC}_2\text{O}_4$ ,  $\text{NH}_4\text{HC}_2\text{O}_4$ , and  $(\text{NH}_4)_2\text{SO}_4/\text{Na}_2\text{C}_2\text{O}_4$  (PDF)

## AUTHOR INFORMATION

### Corresponding Author

\*E-mail: kbeyer@uwlax.edu. Phone: 608-785-8292.

### Notes

The authors declare no competing financial interest.

## ACKNOWLEDGMENTS

We wish to thank Anastasiya Vinokur and Dr. Ilia Guzei at the University of Wisconsin–Madison for running and analyzing the X-ray crystallography experiments and Dr. Kendric Nelson of the UW–La Crosse chemistry department for helpful

discussions on the crystal structural data. This work was supported by the NSF Atmospheric Chemistry Program (AGS-1361592).

## ■ REFERENCES

- Murphy, D. M.; Thomson, D. S.; Mahoney, T. M. J. In Situ Measurements of Organics, Meteoritic Material, Mercury, and Other Elements in Aerosols at 5 to 19 Kilometers. *Science* **1998**, *282*, 1664–1669.
- Froyd, K. D.; Murphy, D. M.; Lawson, P.; Baumgardner, D.; Herman, R. L. Aerosols That Form Subvisible Cirrus at the Tropical Tropopause. *Atmos. Chem. Phys.* **2010**, *10* (1), 209–218.
- Seinfeld, J. H.; Pandis, S. N. *Atmospheric Chemistry and Physics: from Air Pollution to Climate Change*; Wiley: New York, 1998.
- Sullivan, R. C.; Prather, K. A. Investigations of the Diurnal Cycle and Mixing State of Oxalic Acid in Individual Particles in Asian Aerosol Outflow. *Environ. Sci. Technol.* **2007**, *41* (23), 8062–8069.
- Kundu, S.; Kawamura, K.; Kobayashi, M.; Tachibana, E.; Lee, M.; Fu, P. Q.; Jung, J. A Sub-decadal Trend in Diacids in Atmospheric Aerosols in Eastern Asia. *Atmos. Chem. Phys.* **2016**, *16* (2), 585–596.
- Hallquist, M.; Wenger, J. C.; Baltensperger, U.; Rudich, Y.; Simpson, D.; Claeys, M.; Dommen, J.; Donahue, N. M.; George, C.; Goldstein, A. H.; et al. The Formation, Properties and Impact of Secondary Organic Aerosol: Current and Emerging Issues. *Atmos. Chem. Phys.* **2009**, *9* (14), 5155–5236.
- Deshmukh, D. K.; Kawamura, K.; Lazaar, M.; Kunwar, B.; Boreddy, S. K. R. Dicarboxylic Acids, Oxoacids, Benzoic Acid, A-dicarbonyls, WSOC, OC, and Ions in Spring Aerosols from Okinawa Island in the Western North Pacific Rim: Size Distributions and Formation Processes. *Atmos. Chem. Phys.* **2016**, *16* (8), 5263–5282.
- Harris, E.; Sinha, B.; Foley, S.; Crowley, J. N.; Borrmann, S.; Hoppe, P. Sulfur Isotope Fractionation During Heterogeneous Oxidation of SO<sub>2</sub> on Mineral Dust. *Atmos. Chem. Phys.* **2012**, *12* (11), 4867–4884.
- Reitz, P.; Spindler, C.; Mentel, T. F.; Poulain, L.; Wex, H.; Mildenberger, K.; Niedermeier, D.; Hartmann, S.; Clauss, T.; Stratmann, F.; et al. Surface Modification of Mineral Dust Particles by Sulphuric Acid Processing: Implications for Ice Nucleation Abilities. *Atmos. Chem. Phys.* **2011**, *11* (15), 7839–7858.
- Harris, E.; Sinha, B.; van Pinxteren, D.; Tilgner, A.; Fomba, K. W.; Schneider, J.; Roth, A.; Gnauk, T.; Fahrbusch, B.; Mertes, S.; et al. Enhanced Role of Transition Metal Ion Catalysis During In-Cloud Oxidation of SO<sub>2</sub>. *Science* **2013**, *340*, 727–730.
- Kerminen, V.-M.; Teinilä, K.; Hillamo, R.; Pakkanen, T. Substitution of Chloride in Sea-salt Particles by Inorganic and Organic Anions. *J. Aerosol Sci.* **1998**, *29* (8), 929–942.
- Kojima, T.; Buseck, P. R.; Iwasaka, Y.; Matsuki, A.; Trochkin, D. Sulfate-coated Dust Particles in the Free Troposphere over Japan. *Atmos. Res.* **2006**, *82*, 698–708.
- Laskin, A.; Moffet, R. C.; Gilles, M. K.; Fast, J. D.; Zaveri, R. A.; Wang, B.; Nigge, P.; Shuthanandan, J. Tropospheric chemistry of internally mixed sea salt and organic particles: Surprising reactivity of NaCl with weak organic acids. *J. Geophys. Res. A* **2012**, *117* (D15), D15302.
- Reid, J. S.; Koppmann, R.; Eck, T. F.; Eleuterio, D. P. A Review of Biomass Burning Emissions Part II: Intensive Physical Properties of Biomass Burning Particles. *Atmos. Chem. Phys.* **2005**, *5* (3), 799–825.
- Zauscher, M. D.; Wang, Y.; Moore, M. J. K.; Gaston, C. J.; Prather, K. A. Air Quality Impact and Physicochemical Aging of Biomass Burning Aerosols During the 2007 San Diego Wildfires. *Environ. Sci. Technol.* **2013**, *47* (14), 7633–7643.
- Hinz, K.-P.; Trimborn, A.; Weingartner, E.; Henning, S.; Baltensperger, U.; Spengler, B. Aerosol Single Particle Composition at the Jungfraujoch. *J. Aerosol Sci.* **2005**, *36* (1), 123–145.
- Murphy, D. M.; Cziczo, D. J.; Froyd, K. D.; Hudson, P. K.; Matthew, B. M.; Middlebrook, A. M.; Peltier, R. E.; Sullivan, A.; Thomson, D. S.; Weber, R. J. Single-particle Mass Spectrometry of Tropospheric Aerosol Particles. *Journal of Geophysical Research: Atmospheres* **2006**, *111* (D23), D23S32.
- Sullivan, R. C.; Guazzotti, S. A.; Sodeman, D. A.; Prather, K. A. Direct Observations of the Atmospheric Processing of Asian Mineral Dust. *Atmos. Chem. Phys.* **2007**, *7* (5), 1213–1236.
- Cziczo, D. J.; Froyd, K. D.; Hoose, C.; Jensen, E. J.; Diao, M.; Zondlo, M. A.; Smith, J. B.; Twohy, C. H.; Murphy, D. M. Clarifying the Dominant Sources and Mechanisms of Cirrus Cloud Formation. *Science* **2013**, *340*, 1320–1324.
- Ghorai, S.; Wang, B.; Tivanski, A.; Laskin, A. Hygroscopic Properties of Internally Mixed Particles Composed of NaCl and Water-Soluble Organic Acids. *Environ. Sci. Technol.* **2014**, *48* (4), 2234–2241.
- Wang, B.; O'Brien, R. E.; Kelly, S. T.; Shilling, J. E.; Moffet, R. C.; Gilles, M. K.; Laskin, A. Reactivity of Liquid and Semisolid Secondary Organic Carbon with Chloride and Nitrate in Atmospheric Aerosols. *J. Phys. Chem. A* **2015**, *119* (19), 4498–4508.
- Linke, W. F. *Solubilities: Inorganic and Metal Organic Compounds: A Revision and Continuation of the Compilation by A. Seidell*, 4th ed.; Van Nostrand, 1958.
- Stephen, H.; Stephen, T.; Silcock, H. L. *Solubilities of Inorganic and Organic Compounds*; Pergamon Press; Macmillan: Oxford, New York, 1963.
- Kissinger, J. A.; Buttke, L. G.; Vinokur, A. I.; Guzei, I. A.; Beyer, K. D. Solubilities and Glass Formation in Aqueous Solutions of the Sodium Salts of Malonic Acid With and Without Ammonium Sulfate. *J. Phys. Chem. A* **2016**, *120* (21), 3827–3834.
- Schubnell, M. Temperature and Heat Flow Calibration of a DSC-Instrument in the Temperature Range Between -100 and 160 Degrees C. *J. Therm. Anal. Cal.* **2000**, *61*, 91–98.
- Zhang, R.; Wooldridge, P. J.; Abbatt, J. P. D.; Molina, M. J. Physical-Chemistry of the H<sub>2</sub>SO<sub>4</sub>/H<sub>2</sub>O Binary-System at Low-Temperatures - Stratospheric Implications. *J. Phys. Chem.* **1993**, *97*, 7351–7358.
- Lide, D. R. *Handbook of Chemistry and Physics*; CRC Press: Boca Raton, FL, 1993.
- Tellgren, R.; Thomas, J. O.; Olovsson, I. Hydrogen Bond Studies. CX. A Neutron Diffraction and Deformation Electron Density Studie of Sodium Hydrogen Oxalate Monohydrate, NaHC<sub>2</sub>O<sub>4</sub>·H<sub>2</sub>O. *Acta Crystallogr., Sect. B: Struct. Crystallogr. Cryst. Chem.* **1977**, *33*, 3500–3504.
- De Villepin, J.; Novak, A. Spectres De Vibration Des Oxalates Acides De Sodium Effet Isotopique Sur La Liaison Hydrogène. *Spectrochim. Acta A* **1971**, *27*, 1259–1270.
- Jeffrey, G. A.; Parry, G. S. The Crystal Structure of Sodium Oxalate. *J. Am. Chem. Soc.* **1954**, *76* (21), 5283–5286.
- NIST Standard Reference Database 69. *NIST Chemistry WebBook*. <http://webbook.nist.gov> (2016).
- Rozaini, M. Z. H.; Brimblecombe, P. The Solubility Measurements of Sodium Dicarboxylate Salts; Sodium Oxalate, Malonate, Succinate, Glutarate, and Adipate in Water from T = (279.15 to 358.15) K. *J. Chem. Thermodyn.* **2009**, *41* (9), 980–983.
- Hansen, A. R.; Beyer, K. D. Experimentally Determined Thermochemical Properties of the Malonic Acid/water System: Implications for Atmospheric Aerosols. *J. Phys. Chem. A* **2004**, *108*, 3457–3466.
- Li, J.; Xu, S.; Shi, Z. Molecular and Crystal Structure Analysis of an Oxalate-bridged Sodium 2D Polymer: [Na(mu(1,1,2,3)-oxalato)(di-mu(1,1)-H<sub>2</sub>O)](n). *Adv. Mater. Res.* **2011**, *399-401*, 916–920.
- Küppers, H. The Crystal Structure of Ammonium Hydrogen Oxalate Hemihydrate. *Acta Crystallogr., Sect. B: Struct. Crystallogr. Cryst. Chem.* **1973**, *29*, 318–327.
- Keller, H. L.; Küppers, H. The Structure of the Monoclinic Low Temperature Modification of Ammonium Hydrogen Oxalate Hemihydrate. *Acta Crystallogr., Sect. A* **1978**, *34*, S104.
- Robertson, J. H. Ammonium Oxalate Monohydrate: Structure Refinement at 30 K. *Acta Crystallogr.* **1965**, *18* (3), 410–417.
- Hill, A. E.; Distler, E. F. The Solubility of Ammonium Oxalate in Water. *J. Am. Chem. Soc.* **1935**, *57* (11), 2203–2204.

(39) Boldyreva, E. V.; Ahsbahs, H.; Chernyshev, V. V.; Ivashevskaya, S. N.; Oganov, A. R. Effect of Hydrostatic Pressure on the Crystal Structure of Sodium Oxalate: X-ray Diffraction Study and Ab Initio Simulations. *Z. Kristallogr. - Cryst. Mater.* **2006**, *221* (3), 186–197.

(40) Clegg, S. L.; Seinfeld, J. H. Thermodynamic Models of Aqueous Solutions Containing Inorganic Electrolytes and Dicarboxylic Acids at 298.15 K. 2. Systems Including Dissociation Equilibria. *J. Phys. Chem. A* **2006**, *110*, 5718–5734.

(41) Amundson, N. R.; Caboussat, A.; He, J. W.; Martynenko, A. V.; Seinfeld, J. H. A Phase Equilibrium Model for Atmospheric Aerosols Containing Inorganic Electrolytes and Organic Compounds (UHAERO), with Application to Dicarboxylic Acids. *J. Geophys. Res.* **2007**, *112* (D24), D24S13.

(42) Zuend, A.; Marcolli, C.; Booth, A. M.; Lienhard, D. M.; Soonsin, V.; Krieger, U. K.; Topping, D. O.; McFiggans, G.; Peter, T.; Seinfeld, J. H. New and Extended Parameterization of the Thermodynamic Model AIOMFAC: Calculation of Activity Coefficients for Organic-inorganic Mixtures Containing Carboxyl, Hydroxyl, Carbonyl, Ether, Ester, Alkenyl, Alkyl, and Aromatic Functional Groups. *Atmos. Chem. Phys.* **2011**, *11* (17), 9155–9206.

(43) Apelblat, A.; Manzurola, E. Solubility of Oxalic, Malonic, Succinic, Adipic, Maleic, Malic, Citric, and Tartaric-Acids in Water from 278.15-K to 338.15-K. *J. Chem. Thermodyn.* **1987**, *19*, 317–320.